Hindawi Publishing Corporation
Mathematical Problems in Engineering
Volume 2013, Article ID 584252, 9 pages
http://dx.doi.org/10.1155/2013/584252

Research Article

Multiscale Characterization of Sea Clutter by Scale-Dependent Lyapunov Exponent

Jing Hu[1,2] and Jianbo Gao[1,2]

[1] *School of Mechanical Engineering, Guangxi University, 100 Daxue Road, Nanning, Guangxi 530005, China*
[2] *PMB Intelligence LLC, Sunnyvale, CA 94087, USA*

Correspondence should be addressed to Jianbo Gao; jbgao.pmb@gmail.com

Received 13 August 2013; Accepted 10 October 2013

Academic Editor: J. A. Tenreiro Machado

Determining whether sea clutter radar returns are stochastic or deterministic is crucial to the successful modelling of sea clutter as well as to facilitate target detection within sea clutter. Despite extensive studies of sea clutter using distributional analysis, chaos analysis, and fractal analysis, the nature of sea clutter is still not well understood. Realizing that the difficulty in sea clutter modeling is due to the multiscale nature of sea clutter, we employ a new multiscale complexity measure, the scale-dependent Lyapunov exponent (SDLE), to better characterize the nonstationary and multiscale nature of sea clutter. SDLE has been shown to readily characterize major models of complex time series, including deterministic chaos, noisy chaos, stochastic oscillations, random $1/f$ processes, random Levy processes, and complex time series with multiple scaling behaviors. With SDLE, we are able to directly show that sea clutter is not chaotic. More importantly, we find a new scaling law suggesting noisy dynamics for sea clutter. The new scaling law has an interesting interpretation in terms of intrinsic predictability of sea clutter, and provides an excellent new means of detecting targets within sea clutter.

1. Introduction

Sea clutter, the backscatter of the transmitted radar signal by elements of the sea surface such as ocean sprays, capillary waves, wind waves, and swells, is highly complicated. The complexity of the signals comes from two sources, the rough sea surface, sometimes oscillatory, sometimes turbulent, and the multipath propagation of radar backscatter. From Figure 1, it is clear that the signal is not purely random, since the waveform can be fairly smooth on short time scales (Figure 1(a)). However, the signal is highly nonstationary, since the frequency of the signal (Figures 1(a) and 1(b)) and the randomness of the signal (Figures 1(c) and 1(d)) change over time drastically. Therefore, Fourier analysis or deterministic chaotic analysis of sea clutter cannot be effective. From Figure 1(e), where $X_t^{(m)} = (X_{tm-m+1} + \cdots + X_{tm})/m$, it can be concluded that neither autoregressive (AR) models nor textbook fractal models can describe the data. This is because AR modeling requires exponentially decaying autocorrelation (which amounts to $\mathrm{Var}(X_t^{(m)}) \sim m^{-1}$), while fractal modeling requires the variation between $\mathrm{Var}(X_t^{(m)})$ and m to follow a power-law [1]. (To see better the variation of $\mathrm{Var}(X_t^{(m)})$ with m, $\log_2[m^2\,\mathrm{Var}(X_t^{(m)})]$ is plotted against $\log_2 m$ in the figure.) However, neither AR nor true fractal behavior is observed in Figure 1(e).

Understanding of sea clutter will depend not only on finding suitable models to describe the surface scattering but also on knowledge of the complex behavior of the sea [2]. As radars become more complex, to fully utilize their power, it has become increasingly important to accurately model their interaction with environment with ever greater fidelity. Therefore, the study of sea clutter continues to be an important aspect of the development of radar systems.

Over the past several decades, a lot of efforts have been made to study sea clutter. Fundamental studies of sea clutter can be roughly classified into three categories: (i) distributional analysis of sea clutter [3–15], (ii) analysis of sea clutter using fractal theory [1, 16–25], and (iii) analysis of sea clutter using chaos theory [26–37]. Despite these extensive studies, however, the nature of sea clutter is still not well understood. As a result, the important problem of target detection within sea clutter remains to be a tremendous

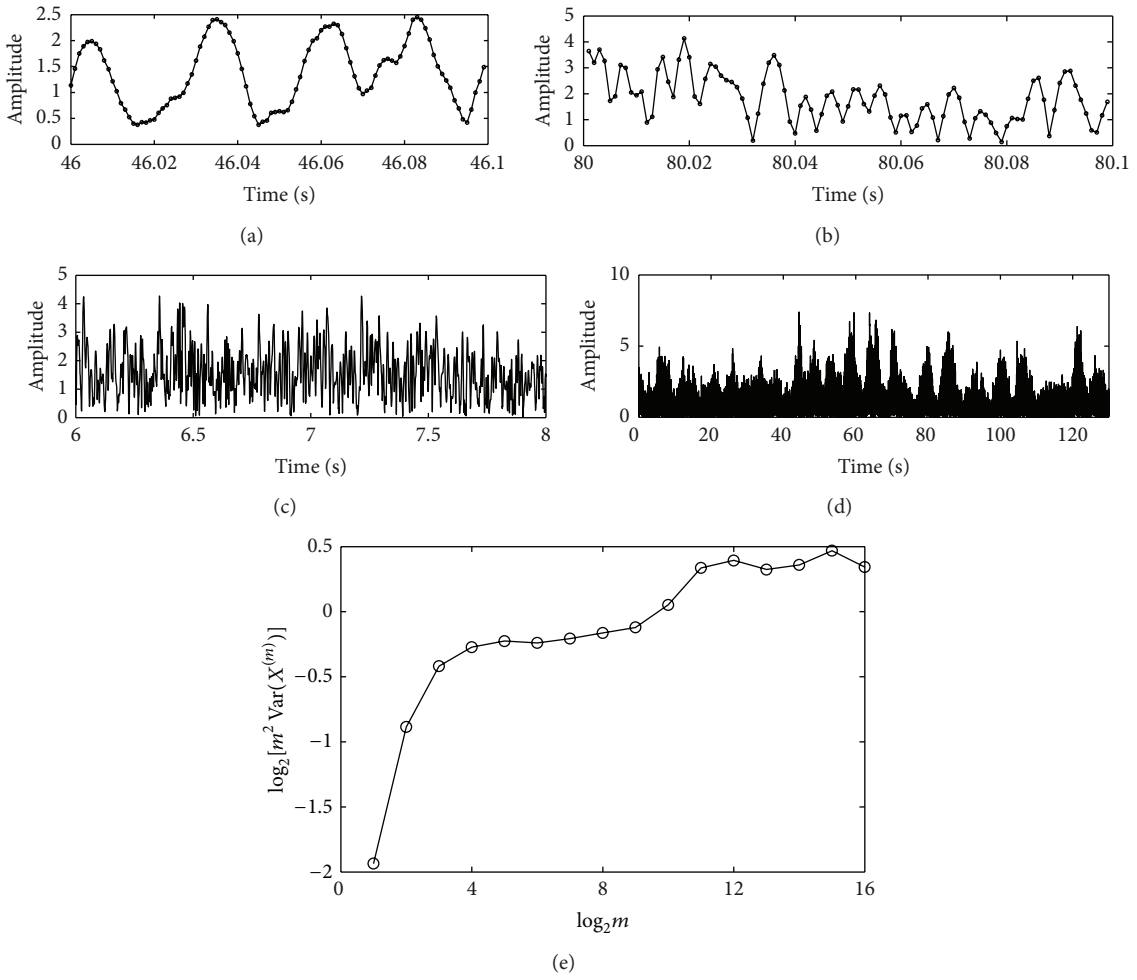

FIGURE 1: ((a) and (b)) Two 0.1 s duration sea clutter signal; (c) a 2 s duration sea clutter signal; (d) the entire sea clutter signal (of about 130 s); and (e) $\log_2[m^2 \mathrm{Var}(X^{(m)}]$ versus $\log_2 m$.

challenge [16, 22, 38–44]. To shed new light on the problem, in this study, we carry out a multiscale analysis of sea clutter, using a recently developed multiscale complexity measure, the scale-dependent Lyapunov exponent (SDLE) [1, 45].

The most salient feature of multiscale signals is that the signals behave differently, depending upon the scale at which the data are examined [1]. To understand why multiscale analysis of sea clutter is essential, it is important to highlight a few empirical observations that point to the multiscale nature of sea clutter: (1) real sea clutter data are highly nonstationary, on both short and long time scales. This has motivated us to fit the differentiated data of sea clutter by Tsallis distribution [13]. (2) In the time scale range of 0.01 to 4 s, structure-function based multifractal characterization detects targets within sea clutter with very high accuracy, although the power-law fractal scaling is not very well defined [1, 23–25]; (3) when analyzed by multiplicative cascade multifractal [35], sea clutter again shows a fractal scaling break on time scales shorter than about 0.01 s. When the envelope of the sea clutter data is extracted by finding all the local maxima and subsequently analyzed, the cascade multifractal characterization becomes excellent; furthermore, log-normal distribution fits the envelope data of sea clutter excellently, but not the original sea clutter data [35]. These observations motivate us to carry out a multiscale analysis of sea clutter by using scale-dependent Lyapunov exponent (SDLE) [1, 45], to shed new light on the nature of sea clutter.

The remainder of the paper is organized as follows. In Section 2, we briefly describe the SDLE, focusing on its properties that are most relevant to sea clutter analysis. In Section 3, we use the SDLE to analyze sea clutter, consider whether such characterization can help detect targets within sea clutter, and compare SDLE with the conventional largest positive Lyapunov exponent. In Section 4, we make a few concluding remarks.

2. SDLE as a Multiscale Complexity Measure

2.1. SDLE: Definition and Computation. SDLE is a recently developed multiscale complexity measure [1, 45]. It has been

used to characterize brainwave EEG data [46, 47], heart rate variability (HRV) [48–51], financial time series [52], Earth's geodynamo [53], among others. SDLE is defined in a phase space through consideration of an ensemble of trajectories [1, 45]. In the case of a scalar time series $x(1), x(2), \ldots, x(n)$, a suitable phase space may be obtained by using time delay embedding [54] to construct vectors of the following form:

$$V_i = [x(i), x(i+L), \ldots, x(i+(m-1)L)], \quad (1)$$

where m and L are called the embedding dimension and the delay time, respectively. For chaotic systems, m and L have to be chosen according to certain optimization criterion [1]. For a stochastic process, which is infinite-dimensional, the embedding procedure transforms a self-affine stochastic process to a self-similar process in a phase space, and often $m = 2$ is sufficient (this issue will be further explained later) [1, 45].

We will now be more concrete. Denote the initial distance between two nearby trajectories by ε_0, and their *average distances* at time t and $t + \Delta t$, respectively, by ε_t and $\varepsilon_{t+\Delta t}$, where Δt is small. The SDLE $\lambda(\varepsilon_t)$ is defined by [1, 45]

$$\varepsilon_{t+\Delta t} = \varepsilon_t e^{\lambda(\varepsilon_t)\Delta t}, \quad \text{or} \quad \lambda(\varepsilon_t) = \frac{\ln \varepsilon_{t+\Delta t} - \ln \varepsilon_t}{\Delta t}. \quad (2)$$

Or equivalently by

$$\frac{d\varepsilon_t}{dt} = \lambda(\varepsilon_t)\varepsilon_t, \quad \text{or} \quad \frac{d \ln \varepsilon_t}{dt} = \lambda(\varepsilon_t). \quad (3)$$

To compute SDLE, we can start from an arbitrary number of shells as follows:

$$\varepsilon_k \le \left\| V_i - V_j \right\| \le \varepsilon_k + \Delta\varepsilon_k, \quad k = 1, 2, 3, \ldots, \quad (4)$$

where V_i and V_j are reconstructed vectors, ε_k (the radius of the shell) and $\Delta\varepsilon_k$ (the width of the shell) are arbitrarily chosen small distances ($\Delta\varepsilon_k$ is not necessarily a constant). Then, we monitor the evolution of all pairs of points (V_i, V_j) within a shell and take average. Equation (2) can now be written as

$$\lambda(\varepsilon_t) = \frac{\left\langle \ln \left\| V_{i+t+\Delta t} - V_{j+t+\Delta t} \right\| - \ln \left\| V_{i+t} - V_{j+t} \right\| \right\rangle}{\Delta t}, \quad (5)$$

where t and Δt are integers in unit of the sampling time, and the angle brackets denote average within a shell. Note that this computational procedure is similar to that for computing the so-called time-dependent exponent curves [55].

Note that the initial set of shells serve as initial values of the scales; through evolution of the dynamics, they will automatically converge to the range of inherent scales. This is emphasized by the subscript t in ε_t, when the scales become inherent, t can then be dropped. Also, note that when analyzing chaotic time series, the following condition:

$$|j - i| \ge (m-1)L \quad (6)$$

needs to be imposed when finding pairs of vectors within a shell, to eliminate the effects of tangential motions [1]. This condition is often also sufficient for an initial scale to converge to the inherent scales [1].

To better understand SDLE, it is instructive to point out a relation between SDLE and the largest positive Lyapunov exponent λ_1 for true chaotic signals. It is given by [1]

$$\lambda_1 = \int_0^{\varepsilon^*} \lambda(\varepsilon)\, p(\varepsilon)\, d\varepsilon, \quad (7)$$

where ε^* is a scale parameter (e.g., used for renormalization when using Wolf et al.'s algorithm [56]), $p(\varepsilon)$ is the probability density function for the scale ε given by

$$p(\varepsilon) = Z\frac{dC(\varepsilon)}{d\varepsilon}, \quad (8)$$

where Z is a normalization constant satisfying $\int_0^{\varepsilon^*} p(\varepsilon)d\varepsilon = 1$ and $C(\varepsilon)$ is the well-known Grassberger-Procaccia's correlation integral [57].

SDLE has distinctive scaling laws for different types of time series. Those most relevant to sea clutter analysis are listed here.

(1) For clean chaos on small scales, and noisy chaos with weak noise on intermediate scales,

$$\lambda(\varepsilon) = \lambda_1. \quad (9)$$

As an operational definition for chaos, we define chaos to be observing scaling of (9) on a scale range of $(\varepsilon, r\varepsilon)$, where $r > 1$ is a coefficient [1, 45]. When low-dimensional chaos is concerned, one may require $r \ge 2$.

(2) For clean chaos on large scales where memory has been lost and for noisy chaos (including noise-induced chaos [58–60]) on small scales,

$$\lambda(\varepsilon) \sim -\gamma \ln \varepsilon, \quad (10)$$

where $\gamma > 0$ is a parameter.

(3) For random $1/f^{2H+1}$ processes, where $0 < H < 1$ is called the Hurst parameter which characterizes the correlation structure of the process: depending on whether H is smaller than, equal to, or larger than 1/2, the process is said to have antipersistent, short-range, or persistent long-range correlations [1, 23] as follows:

$$\lambda(\varepsilon) \sim \varepsilon^{-1/H}. \quad (11)$$

Note that $H = 1/2$ for the standard Brownian motion and $H = 1/3$ for turbulence. Note also that this scaling is quite independent of m, except that the scale range defining (11) shrinks when m increases. Because of this, $m = 2$ again is preferred.

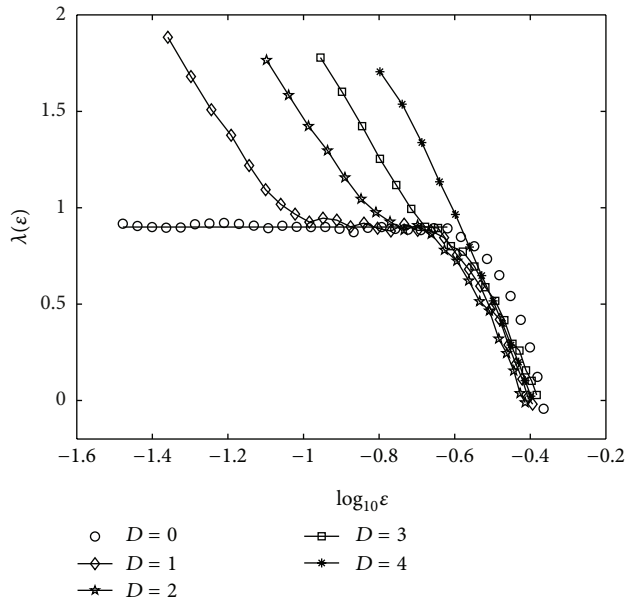

FIGURE 2: $\lambda(\varepsilon)$ curves for the clean and the noisy Lorenz system.

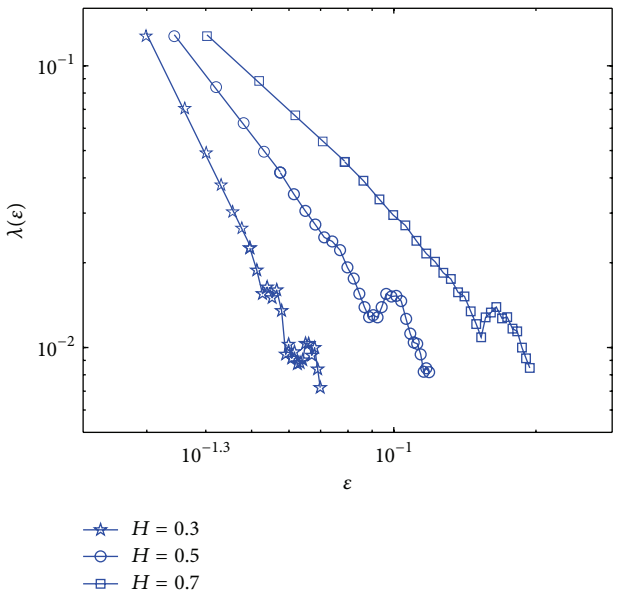

FIGURE 3: $\lambda(\varepsilon)$ versus ε curves for perturbed $1/f$ processes. Curves for three different H are plotted. To put all the curves on one plot, the curves for different H (except the smallest one considered here) are arbitrarily shifted rightward.

To better appreciate the above properties, it is helpful to examine the chaotic Lorenz system with stochastic forcing as an example as follows:

$$\begin{aligned} \frac{dx}{dt} &= -10(x-y) + D\eta_1(t), \\ \frac{dy}{dt} &= -xz + 28x - y + D\eta_2(t), \\ \frac{dz}{dt} &= xy - \frac{8}{3}z + D\eta_3(t), \end{aligned} \tag{12}$$

where $D\eta_i(t)$, $i = 1, 2, 3$ are independent Gaussian noise forcing terms with mean 0 and variance D^2. Note that the system with a different parameter set was studied in [1, 45]. The system is solved using the scheme of Exact propagator [61], where the exact solution of the Lorenz system is solved using a 4th order Runge-Kutta method with a time-step of $h = 0.002$, and then a term $D\sqrt{h}W$, where W is a Gaussian noise of mean 0 and variance 1, is added to the corresponding equations to take into account the noise. Figure 2 shows five curves, for the cases of $D = 0, 1, 2, 3, 4$. The computations are done using $m = 4$, $L = 2$, and 10000 points of the x component of the Lorenz system sampled at a time interval of 0.06. For the clean system, we observe two scaling laws. One is (9), $\lambda(\varepsilon) \approx 0.9$, for small ε, the other is (10), for large ε where memory has been lost. For the noisy system, the scale region where the scaling law of (9) shrinks when the stochastic forcing is increased. Interestingly, although the part of the curve with $\lambda(\varepsilon) \sim -\gamma \ln \varepsilon$ shifts to the right when noise is increased, the parameter γ appears to not depend on the noise strength.

2.2. Coping with Nonstationarity. Since sea clutter is nonstationary [1, 13], it is important to understand how SDLE deals with nonstationarity before it is used to analyze sea clutter. Noting that sea clutter has fractal $1/f$ scaling behavior in the time scale range from 0.01 to 4 s [1, 23–25], we first study if the $1/f$ feature remains robust under the following perturbations.

(1) Shift a $1/f^\beta$, $\beta = 2H+1$ process downward or upward at randomly chosen points in time by an arbitrary amount. For convenience, we call this procedure type 1 nonstationarity and the processes obtained broken-$1/f^\beta$ processes.

(2) At randomly chosen time intervals, concatenate randomly broken-$1/f^\beta$ processes and oscillatory components or superimpose oscillatory components on broken-$1/f^\beta$ processes. This procedure causes a different type of nonstationarity, which for convenience we will call type 2 nonstationarity.

We call the resulting random processes perturbed $1/f^\beta$ processes. Three examples of the $\lambda(\varepsilon)$ curves for such processes, where the frequency of the perturbations are, on average, 1% of the simulated data, are shown in Figure 3. We observe that (11) still holds very well when $\lambda(\varepsilon) > 0.02$. Therefore, SDLE can readily characterize $1/f$ processes perturbed by either of the nonstationarities considered.

To understand why the SDLE can deal with type 1 nonstationarity, it suffices to note that type 1 nonstationarity causes shifts of the trajectory in phase space; the greater the nonstationarity, the larger the shifts. The SDLE, however, cannot be affected much by shifts, especially large ones, since it is based on the coevolution of pairs of vectors within chosen small shells. In fact, the effect of shifts is to exclude a few pairs of vectors that were originally counted in the ensemble

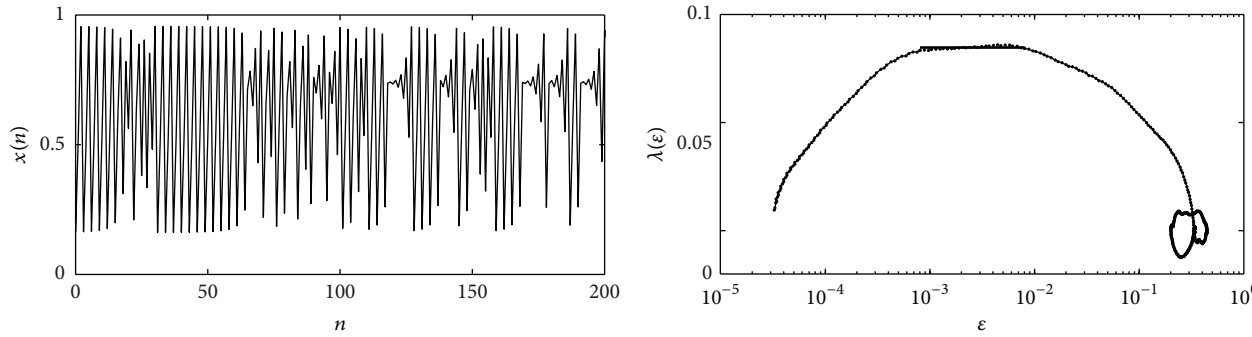

Figure 4: (a) An intermittent time series generated by the logistic map. (b) The SDLE curve for the time series.

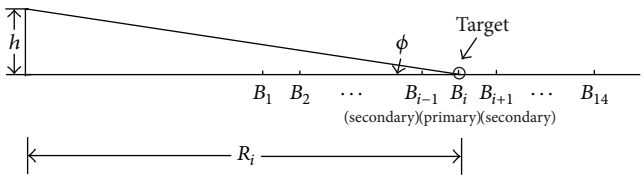

Figure 5: A schematic showing how the sea clutter data were collected.

average. Therefore, so long as the shifts are not too frequent, the effect of shifts can be neglected, since ensemble average within a shell involves a large number of pairs of vectors.

Let us now turn to type 2 nonstationarity, which involves oscillatory components. Being regular, oscillatory components can only affect $\lambda(\varepsilon)$ where it is close to 0. Therefore, type 2 nonstationarity cannot affect the positive portion of $\lambda(\varepsilon)$ either.

Note that similar types of perturbations have been carried out to clean and noisy chaotic data, and the major features of (9) and (10) are also robust, as expected.

Finally, we examine whether SDLE can detect chaos from an intermittent time series with a long laminar phase during which neighboring trajectories do not diverge, and a rapid divergence over a small part of the state space. Such a case is most relevant to the transitions from a quiet sea surface to a turbulent sea disturbed by a sudden gust of wind, and vice versa. For this purpose, we study the logistic map as follows:

$$x_{n+1} = a x_n (1 - x_n), \quad a = 3.8284. \tag{13}$$

Figure 4(a) shows an intermittent time series. We note that the chaotic part is very short compared with the periodic part. Figure 4(b) shows the SDLE curve for the time series. We clearly observe a plateau defining a chaotic motion. Also, note that the $\ln \varepsilon$ scaling on very small scales indicates the transitions from periodic to chaotic motions, and vice versa (it is unstable, but not chaotic in the rigorous sense).

3. Multiscale Analysis of Sea Clutter

3.1. Sea Clutter Data. Fourteen sea clutter datasets were obtained from a website maintained by Professor Simon Haykin: http://soma.ece.mcmaster.ca/ipix/dartmouth/datasets.html.

The measurement was made using the McMaster IPIX radar at Dartmouth, Nova Scotia, Canada. The radar was mounted in a fixed position on land 25–30 m above sea level, with an operating (carrier) frequency of 9.39 GHz (and hence a wavelength of about 3 cm). It was operated at low grazing angles, with the antenna dwelling in a fixed direction, illuminating a patch of ocean surface. The measurements were performed with the wave height in the ocean varying from 0.8 to 3.8 m (with peak heights up to 5.5 m) and the wind conditions varying from still to 60 km/hr (with gusts up to 90 km/hr). For each measurement, 14 areas, called antenna footprints or range bins, were scanned. Their centers are depicted as $B_1, B_2, \ldots, B_{14}$ in Figure 5. The distance between two adjacent range bins was 15 m. One or a few range bins (say, B_{i-1}, B_i and B_{i+1}) hit a target, which was a spherical block of styrofoam of diameter 1 m wrapped with wire mesh. The locations of the three targets were specified by their azimuthal angle and distance to the radar. They were (128^0, 2660 m), (130^0, 5525 m), and (170^0, 2655 m), respectively. The range bin where the target is strongest is labeled as the primary target bin. Due to the drift of the target, bins adjacent to the primary target bin may also have hit the target. They are called secondary target bins. For each range bin, there were 2^{17} complex numbers, sampled with a frequency of 1000 Hz.

3.2. Sea Clutter Analysis. The SDLE curves can be readily computed from sea clutter data. Figure 6(a) shows a typical example. We do not observe the chaotic scaling of (9) on any significant scale ranges. Therefore, sea clutter is not chaotic. While this result is consistent with the results of [29, 30, 33–37], it merits noting that the SDLE method is a direct method and is more rigorous.

More interestingly, all the sea clutter data, whether it is with target or without target, yields the scaling of (10). Therefore, (10) describes a prevailing feature of sea clutter. To understand which feature that is as well as to understand

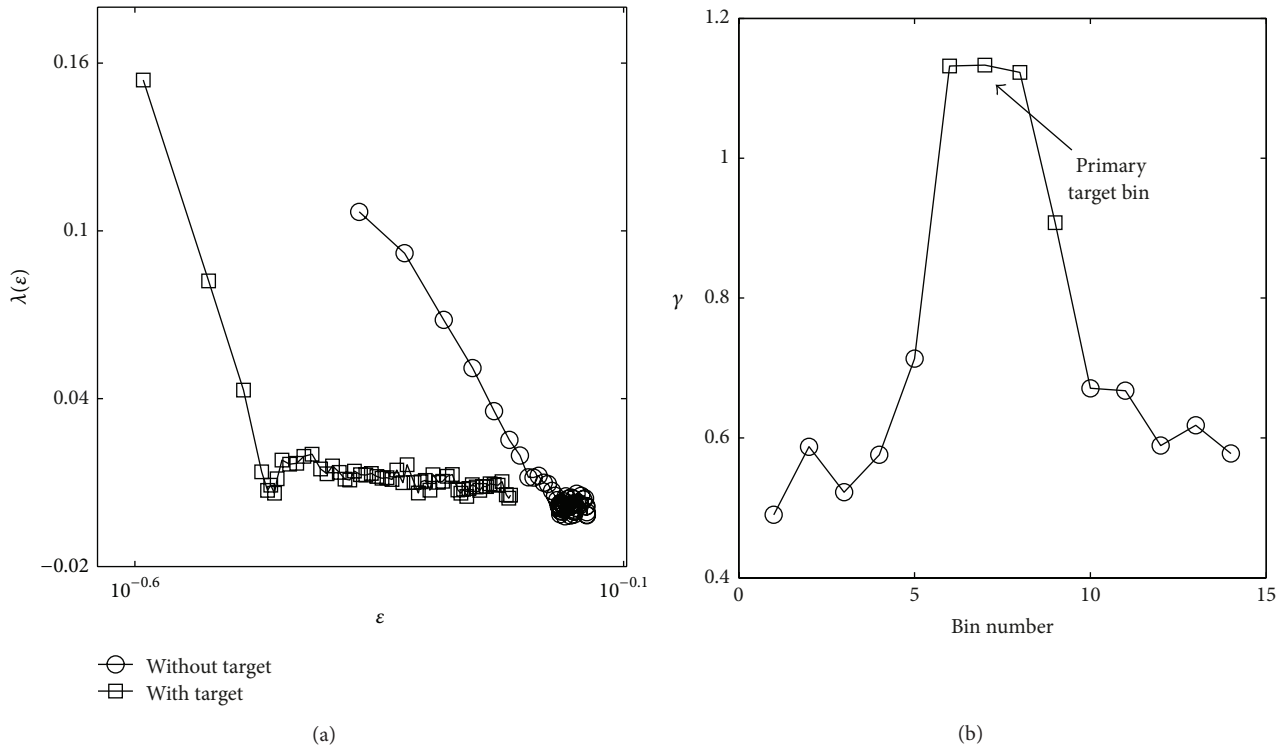

FIGURE 6: (a) $\lambda(\varepsilon)$ curves for sea clutter. The embedding parameters are $m = 4$, $L = 1$. (b) Target detection using γ parameter.

the physical significance of γ, let us consider the problem of predictability with sea clutter. Specifically, we consider the concept of the error *doubling time*, defined as the average time for an initial error ε_0 to double: an error grows faster when the doubling time is shorter. In other words, a faster error growth means a more rapid loss of initial information.

What is the error doubling time for sea clutter data? To find this, we use (3) to get the following:

$$\ln \varepsilon_t = \ln \varepsilon_0 + \int_0^t \lambda\left(\varepsilon_t\right) dt. \tag{14}$$

Letting $\varepsilon_{T_{db}} = 2\varepsilon_0$, we find the error doubling time T_{db} given by

$$\ln 2 = \int_0^{T_{db}} \lambda\left(\varepsilon_t\right) dt. \tag{15}$$

As the first approximation, we may consider $1/\lambda(\varepsilon)$ to be proportional to the doubling time. When $\lambda(\varepsilon)$ is given by (10), then the error doubling time is inversely proportional to γ. Therefore, γ characterizes the speed of information loss. More rigorously, we can prove that $-\ln \varepsilon_0 \gg 1$ decays to a saturation or limiting value of 0 exponentially as follows:

$$-\ln \varepsilon_t = -\ln \varepsilon_0 e^{-\gamma t}. \tag{16}$$

A zero magnitude of $\ln \varepsilon_t$ amounts to a unit error. Therefore, it is proper to call γ the relaxation parameter of information loss. The fact that γ is larger for sea clutter with target implies that information loss in sea clutter with target is faster. Physically, this may be attributed to the generation of turbulence near the target.

Can the γ parameter be used to help detect targets within sea clutter? The answer is positive, as shown in Figure 6(b). Clearly, γ is very effective in distinguishing sea clutter with and without targets. For automatic detection purposes, we have analyzed almost 400 datasets available to us and found that a threshold value of 0.9 for γ yields an almost perfect classification as follows.

(i) Hypothesis H_0: sea clutter without target, $\gamma < 0.9$.

(ii) Hypothesis H_1: sea clutter with target, $\gamma \geq 0.9$.

When a signal is truly chaotic, SDLE is related to the conventional positive Lyapunov exponent by (7). Now that we have found sea clutter not to be chaotic, it is interesting to find out how different SDLE is from λ_1. We have computed λ_1 for all the sea clutter data using Wolf et al.'s algorithm [56]. Wolf et al.'s algorithm works as follows: one selects a reference trajectory and follows the divergence of its neighboring trajectory from it. Denote the reference and the neighboring trajectories by $X_i = [x(i), x(i + L), \ldots, x(i + (m - 1)L)]$, $X_j = [x(j), x(j + L), \ldots, x(j + (m - 1)L)]$, $i = 1, 2, \ldots$, and $j = K, K + 1, \ldots$, respectively. At the start of the time (which corresponds to $i = 1$), X_K is usually taken as the nearest neighbor of X_1. That is, $j = K$ minimizes the distance between X_j and X_1. When time evolves, the distance between X_i and X_j also changes. Let the spacing between the two trajectories at time t_i and t_{i+1} be d_i' and d_{i+1}, respectively.

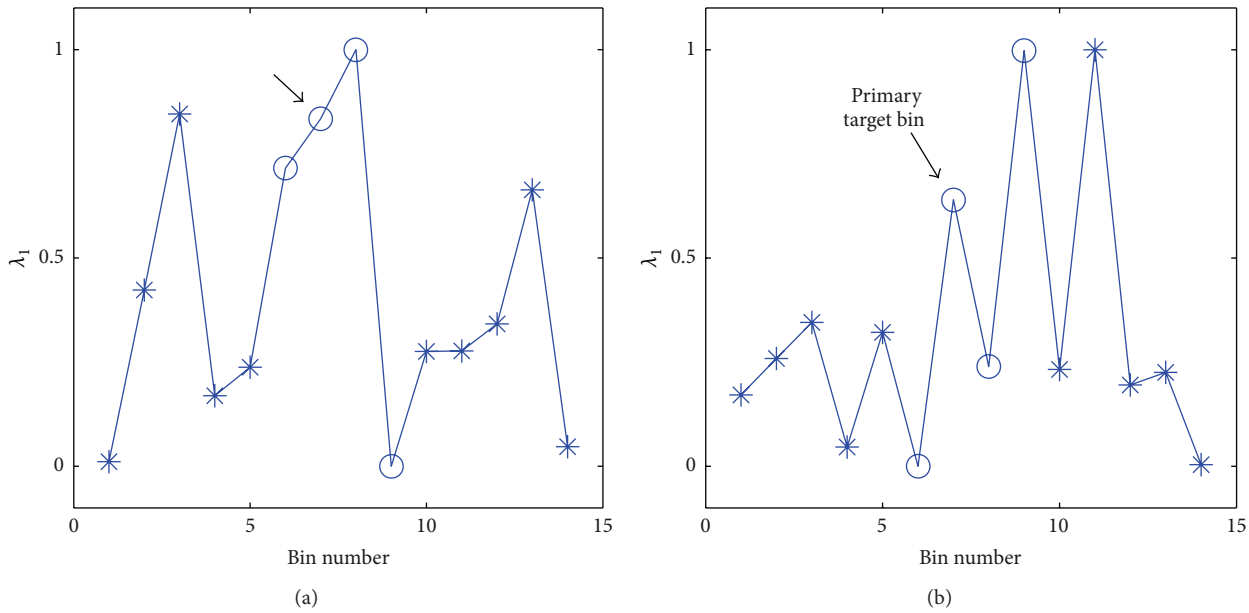

FIGURE 7: ((a) and (b)) The variations of the Lyapunov exponent λ estimated by conventional methods versus the 14 range bins for two HH measurements. Open circles denote the range bins with target, while asterisks denote the bins without target. The primary target bin is explicitly indicated by an arrow. For convenience, the largest λ_c is taken as 1 unit.

Assuming that $d_{i+1} \sim d_i' e^{\lambda_1 (t_{i+1} - t_i)}$, the rate of divergence of the trajectory, λ_1, over a time interval of $t_{i+1} - t_i$ is then

$$\frac{\ln\left(d_{i+1}/d_i'\right)}{t_{i+1} - t_i}. \tag{17}$$

To ensure that the separation between the two trajectories is always small, when d_{i+1} exceeds certain threshold value, it has to be renormalized; a new point in the direction of the vector of d_{i+1} is picked up so that d_{i+1}' is very small compared to the size of the attractor. After n repetitions of stretching and renormalizing the spacing, one obtains the following formula:

$$\begin{aligned} \lambda_1 &= \sum_{i=1}^{n-1} \left[\frac{t_{i+1} - t_i}{\sum_{i=1}^{n-1} \left(t_{i+1} - t_i\right)} \right] \left[\frac{\ln\left(d_{i+1}/d_i'\right)}{t_{i+1} - t_i} \right] \\ &= \frac{\sum_{i=1}^{n-1} \ln\left(d_{i+1}/d_i'\right)}{t_n - t_1}. \end{aligned} \tag{18}$$

Figures 7(a) and 7(b) show representative λ_1 for two measurements, where the largest λ_1 among the 14 bins of a measurement is taken as 1 unit. Clearly, λ_1 does not have any power of detecting targets within sea clutter. This suggests that λ_1 only characterizes noise in sea clutter, whether they hit targets or not. Therefore, the effectiveness of using (10) to detect targets within sea clutter suggests that SDLE is fundamentally different from the conventional Lyapunov exponent.

4. Concluding Remarks

To better characterize the nonstationary and multiscale nature of sea clutter, in this study, we have employed SDLE to analyze low-grazing angle sea clutter. We are able to directly show that sea clutter is not chaotic and reveal a new scaling law suggesting noisy dynamics for sea clutter. The new scaling law has an interesting interpretation in terms of intrinsic predictability of sea clutter. The fact that it can be used to accurately detect targets within sea clutter implies that it is a fundamental feature of sea clutter.

References

[1] J. B. Gao, Y. H. Cao, W. W. Tung, and J. Hu, *Multiscale Analysis of Complex Time Series: Integration of Chaos and Random Fractal Theory, and Beyond*, John Wiley & Sons, Hoboken, NJ, USA, 2007.

[2] L. B. Wetzel, "Sea clutter," in *Radar Handbook*, M. I. Skolnik, Ed., chapter 13, McGraw-Hill, New York, NY, USA, 2nd edition, 1990.

[3] F. A. Fay, J. Clarke, and R. S. Peters, "Weibull distribution applied to sea-clutter," in *Proceedings of the IEE International Radar'77 Conference*, pp. 101–104, London, UK, October 1977.

[4] F. E. Nathanson, *Radar Design Principles*, McGraw-Hill, New York, NY, USA, 1969.

[5] G. V. Trunk and S. F. George, "Detection of targets in non-Gaussian sea clutter," *IEEE Transactions on Aerospace and Electronic Systems*, vol. 6, no. 5, pp. 620–628, 1970.

[6] H. C. Chan, "Radar sea-clutter at low grazing angles," *IEE Proceedings F*, vol. 137, no. 2, pp. 102–112, 1990.

[7] E. Jakeman and P. N. Pusey, "A model for non-Rayleigh sea echo ," *IEEE Transactions on Antennas and Propagation*, vol. 24, no. 6, pp. 806–814, 1976.

[8] K. D. Ward, C. J. Baker, and S. Watts, "Maritime surveillance radar—part 1: radar scattering from the ocean surface," *IEE Proceedings F*, vol. 137, no. 2, pp. 51–62, 1990.

[9] T. J. Nohara and S. Haykin, "Canadian east coast radar trials and the *K*-distribution," *IEE Proceedings F*, vol. 138, no. 2, pp. 80–88, 1991.

[10] S. Sayama and M. Sekine, "Log-normal, log-Weibull and K-distributed sea clutter," *IEICE Transactions on Communications*, vol. 85, no. 7, pp. 1375–1381, 2002.

[11] F. Gini, "Performance analysis of two structured covariance matrix estimators in compound-Gaussian clutter," *Signal Processing*, vol. 80, no. 2, pp. 365–371, 2000.

[12] R. J. A. Tough and K. D. Ward, "Diffusive and related models of some properties of sea clutter," *Journal of Physics Condensed Matter*, vol. 14, no. 33, pp. 7737–7748, 2002.

[13] J. Hu, W. W. Tung, and J. B. Gao, "A new way to model nonstationary sea clutter," *IEEE Signal Processing Letters*, vol. 16, no. 2, pp. 129–132, 2009.

[14] F. Gini, M. Montanari, and L. Verrazzani, "Maximum likelihood, ESPRIT, and periodogram frequency estimation of radar signals in K-distributed clutter," *Signal Processing*, vol. 80, no. 6, pp. 1115–1126, 2000.

[15] F. Geni, A. Farina, and M. Montanari, "Vector subspace detection in compound-Gaussian clutter part II: performance analysis," *IEEE Transactions on Aerospace and Electronic Systems*, vol. 38, no. 4, pp. 1312–1323, 2002.

[16] M. Martorella, F. Berizzi, and E. D. Mese, "On the fractal dimension of sea surface backscattered signal at low grazing angle," *IEEE Transactions on Antennas and Propagation*, vol. 52, no. 5, pp. 1193–1204, 2004.

[17] J. Chen, T. K. Y. Lo, H. Leung, and J. Litva, "The use of fractals for modeling EM waves scattering from rough sea surface," *IEEE Transactions on Geoscience and Remote Sensing*, vol. 34, no. 4, pp. 966–972, 1996.

[18] F. Berizzi, E. Dalle Mese, and M. Martorella, "A sea surface fractal model for ocean remote sensing," *International Journal of Remote Sensing*, vol. 25, no. 7-8, pp. 1265–1270, 2004.

[19] F. Berizzi and E. Dalle-Mese, "Scattering from a 2-D sea fractal surface: fractal analysis of the scattered signal," *IEEE Transactions on Antennas and Propagation*, vol. 50, no. 7, pp. 912–925, 2002.

[20] G. Franceschetti, A. Iodice, M. Migliaccio, and D. Riccio, "Scattering from natural rough surfaces modeled by fractional Brownian motion two-dimensional processes," *IEEE Transactions on Antennas and Propagation*, vol. 47, no. 9, pp. 1405–1415, 1999.

[21] T. Lo, H. Leung, J. Litva, and S. Haykin, "Fractal characterization of sea-scattered signals and detection of sea-surface targets," *IEE Proceedings F*, vol. 140, no. 4, pp. 243–250, 1993.

[22] C. P. Lin, M. Sano, S. Sayama, and M. Sekine, "Detection of radar targets embedded in sea ice and sea clutter using fractals, wavelets, and neural networks," *IEICE Transactions on Communications*, vol. 83, no. 9, pp. 1916–1929, 2000.

[23] J. B. Gao, J. Hu, W. W. Tung, Y. H. Cao, N. Sarshar, and V. P. Roychowdhury, "Assessment of long-range correlation in time series: how to avoid pitfalls," *Physical Review E*, vol. 73, no. 1, Article ID 016117, 2006.

[24] J. Hu, J. B. Gao, F. L. Posner, Y. I. Zheng, and W. W. Tung, "Target detection within sea clutter: a comparative study by fractal scaling analyses," *Fractals*, vol. 14, no. 3, pp. 187–204, 2006.

[25] J. Hu, W. W. Tung, and J. B. Gap, "Detection of low observable targets within sea clutter by structure function based multifractal analysis," *IEEE Transactions on Antennas and Propagation*, vol. 54, no. 1, pp. 136–143, 2006.

[26] S. Haykin and S. Puthusserypady, "Chaotic dynamics of sea clutter," *Chaos*, vol. 7, no. 4, pp. 777–802, 1997.

[27] S. Haykin, *Chaotic Dynamics of Sea Clutter*, vol. 17 of *Adaptive and Learning Systems for Signal Processing, Communications, and Control*, John Wiley & Sons, Hoboken, NJ, USA, 1999.

[28] S. Haykin, R. Barker, and B. W. Currie, "Uncovering nonlinear dynamics-the case study of sea clutter," *Proceedings of the IEEE*, vol. 90, no. 5, pp. 860–881, 2002.

[29] M. Davies, "Looking for non-linearities in sea clutter," in *Proceedings of the IEE Radar and Sonar Signal Processing*, Peebles, UK, July 1998.

[30] M. R. Cowper, B. Mulgrew, and C. P. Unsworth, "Investigation into the use of nonlinear predictor networks to improve the performance of maritime surveillance radar target detectors," *IEE Proceedings—Radar, Sonar and Navigation*, vol. 148, no. 3, pp. 103–111, 2001.

[31] M. R. Cowper and B. Mulgrew, "Nonlinear processing of high resolution radar sea clutter," in *Proceedings of the International Joint Conference on Neural Networks (IJCNN '99)*, pp. 2633–2638, July 1999.

[32] J. L. Noga, *Bayesian state-space modelling of spatio-temporal non-Gaussian radar returns [Ph.D. thesis]*, Cambridge University, 1998.

[33] C. P. Unsworth, M. R. Cowper, S. McLaughlin, and B. Mulgrew, "False detection of chaotic behavior in the stochastic compound k-distribution model of radar sea clutter," in *Proceedings of the 10th IEEE Workshop on Statistical Signal and Array Processing (SSAP '00)*, pp. 296–300, August 2000.

[34] C. P. Unsworth, M. R. Cowper, S. McLaughlin, and B. Mulgrew, "Re-examining the nature of radar sea clutter," *IEE Proceedings—Radar, Sonar and Navigation*, vol. 149, no. 3, pp. 105–114, 2002.

[35] J. B. Gao and K. Yao, "Multifractal features of sea clutter," in *Proceedings of the IEEE Radar Conference*, pp. 500–505, Long Beach, Calif, USA, April 2002.

[36] J. B. Gao, S. K. Hwang, H. F. Chen, Z. Kang, K. Yao, and J. M. Liu, "Can sea clutter and indoor radio propagation be modeled as strange attractors?" in *Proceedings of the 7th Experimental Chaos Conference*, vol. 676, pp. 154–161, San Diego, Calif, USA, August 2002.

[37] M. McDonald and A. Damini, "Limitations of nonlinear chaotic dynamics in predicting sea clutter returns," *IEE Proceedings—Radar, Sonar and Navigation*, vol. 151, no. 2, pp. 105–113, 2004.

[38] T. Thayaparan and S. Kennedy, "Detection of a manoeuvring air target in sea-clutter using joint time-frequency analysis techniques," *IEE Proceedings—Radar, Sonar and Navigation*, vol. 151, no. 1, pp. 19–30, 2004.

[39] G. Davidson and H. D. Griffiths, "Wavelet detection scheme for small targets in sea clutter," *Electronics Letters*, vol. 38, no. 19, pp. 1128–1130, 2002.

[40] T. K. Bhattacharya and S. Haykin, "Neural network-based adaptive radar detection scheme for small ice targets in sea clutter," *Electronics Letters*, vol. 28, no. 16, pp. 1528–1529, 1992.

[41] T. K. Bhattacharya and S. Haykin, "Neural network-based radar detection for an ocean environment," *IEEE Transactions on Aerospace and Electronic Systems*, vol. 33, no. 2, pp. 408–420, 1997.

[42] H. Leung, N. Dubash, and N. Xie, "Detection of small objects in clutter using a GA-RBF neural network," *IEEE Transactions on Aerospace and Electronic Systems*, vol. 38, no. 1, pp. 98–118, 2002.

[43] N. Xie, H. Leung, and H. Chan, "A multiple-model prediction approach for sea clutter modeling," *IEEE Transactions on Geoscience and Remote Sensing*, vol. 41, no. 6, pp. 1491–1502, 2003.

[44] C. P. Lin, M. Sano, S. Obi, S. Sayama, and M. Sekine, "Detection of oil leakage in SAR images using wavelet feature extractors and unsupervised neural classifiers," *IEICE Transactions on Communications*, vol. 83, no. 9, pp. 1955–1962, 2000.

[45] J. B. Gao, J. Hu, W. W. Tung, and Y. H. Cao, "Distinguishing chaos from noise by scale-dependent Lyapunov exponent," *Physical Review E*, vol. 74, no. 6, Article ID 066204, 9 pages, 2006.

[46] J. B. Gao, J. Hu, and W. W. Tung, "Complexity measures of brain wave dynamics," *Cognitive Neurodynamics*, vol. 5, no. 2, pp. 171–182, 2011.

[47] J. B. Gao, J. Hu, and W. W. Tung, "Entropy measures for biological signal analyses," *Nonlinear Dynamics*, vol. 68, no. 3, pp. 431–444, 2012.

[48] J. Hu, J. B. Gao, W. W. Tung, and Y. H. Cao, "Multiscale analysis of heart rate variability: a comparison of different complexity measures," *Annals of Biomedical Engineering*, vol. 38, no. 3, pp. 854–864, 2010.

[49] J. Hu, J. B. Gao, and W. W. Tung, "Characterizing heart rate variability by scale-dependent Lyapunov exponent," *Chaos*, vol. 19, no. 2, Article ID 028506, 6 pages, 2009.

[50] J. B. Gao, J. Hu, W. W. Tung, and E. Blasch, "Multiscale analysis of physiological data by scale-dependent Lyapunov exponent," *Frontiers in Fractal Physiology*, 2012.

[51] J. B. Gao, B. M. Gurbaxani, J. Hu et al., "Multiscale analysis of heart rate variability in nonstationary environments," *Frontiers in Computational Physiology and Medicine*, 2013.

[52] J. B. Gao, J. Hu, W. W. Tung, and Y. Zheng, "Multiscale analysis of economic time series by scale-dependent Lyapunov exponent," *Quantitative Finance*, vol. 13, no. 2, pp. 265–274, 2013.

[53] D. A. Ryan and G. R. Sarson, "The geodynamo as a low-dimensional deterministic system at the edge of chaos," *Europhysics Letters*, vol. 83, no. 4, Article ID 49001, 6 pages, 2008.

[54] F. Takens, "Detecting strange attractors in turbulence," in *Dynamical Systems and Turbulence*, D. A. Rand and L. S. Young, Eds., vol. 898 of *Lecture Notes in Mathematics*, pp. 366–381, Springer, Berlin, Germany, 1981.

[55] J. B. Gao and Z. M. Zheng, "Direct dynamical test for deterministic chaos and optimal embedding of a chaotic time series," *Physical Review E*, vol. 49, no. 5, pp. 3807–3814, 1994.

[56] A. Wolf, J. B. Swift, H. L. Swinney, and J. A. Vastano, "Determining Lyapunov exponents from a time series," *Physica D*, vol. 16, no. 3, pp. 285–317, 1985.

[57] P. Grassberger and I. Procaccia, "Characterization of strange attractors," *Physical Review Letters*, vol. 50, no. 5, pp. 346–349, 1983.

[58] J. B. Gao, S. K. Hwang, and J. M. Liu, "When can noise induce chaos?" *Physical Review Letters*, vol. 82, no. 6, pp. 1132–1135, 1999.

[59] J. B. Gao, G. C. Chen, S. K. Hwang, and J. M. Liu, "Noise-induced chaos," *International Journal of Modern Physics B*, vol. 13, no. 28, pp. 3283–3305, 1999.

[60] S. K. Hwang, J. B. Gao, and J. M. Liu, "Noise-induced chaos in an optically injected semiconductor laser model," *Physical Review E*, vol. 61, no. 5, pp. 5162–5170, 2000.

[61] R. Mannella, "Integration of stochastic differential equations on a computer," *International Journal of Modern Physics C*, vol. 13, no. 9, pp. 1177–1194, 2002.